Korean J Physiol Pharmacol 2019;23(4):281-289
https://doi.org/10.4196/kjpp.2019.23.4.281

KJPP

Original Article

Increased expression of vascular endothelial growth factor-C and vascular endothelial growth factor receptor-3 after pilocarpine-induced status epilepticus in mice

Kyung-Ok Cho[1,2,3,4,#], Joo Youn Kim[1,#], Kyoung Hoon Jeong[1], Mun-Yong Lee[2,3,5], and Seong Yun Kim[1,2,3,*]

[1]Department of Pharmacology, College of Medicine, The Catholic University of Korea, [2]Department of Biomedicine & Health Sciences, The Catholic University of Korea, [3]Catholic Neuroscience Institute, [4]Institute of Aging and Metabolic Diseases, [5]Department of Anatomy, College of Medicine, The Catholic University of Korea, Seoul 06591, Korea

ARTICLE INFO

Received April 14, 2019
Revised May 7, 2019
Accepted May 8, 2019

***Correspondence**
Seong Yun Kim
E-mail: syk@catholic.ac.kr

Key Words
Hippocampus
Mouse
Vascular endothelial growth factor-C
Vascular endothelial growth factor receptor-3
Status epilepticus

[#]These authors contributed equally to this work.

ABSTRACT Vascular endothelial growth factor (VEGF)-C and its receptor, vascular endothelial growth factor receptor (VEGFR)-3, are responsible for lymphangiogenesis in both embryos and adults. In epilepsy, the expression of VEGF-C and VEGFR-3 was significantly upregulated in the human brains affected with temporal lobe epilepsy. Moreover, pharmacologic inhibition of VEGF receptors after acute seizures could suppress the generation of spontaneous recurrent seizures, suggesting a critical role of VEGF-related signaling in epilepsy. Therefore, in the present study, the spatiotemporal expression of VEGF-C and VEGFR-3 against pilocarpine-induced status epilepticus (SE) was investigated in C57BL/6N mice using immunohistochemistry. At 1 day after SE, hippocampal astrocytes and microglia were activated. Pyramidal neuronal death was observed at 4 days after SE. In the subpyramidal zone, VEGF-C expression gradually increased and peaked at 7 days after SE, while VEGFR-3 was significantly upregulated at 4 days after SE and began to decrease at 7 days after SE. Most VEGF-C/VEGFR-3-expressing cells were pyramidal neurons, but VEGF-C was also observed in some astrocytes in sham-manipulated animals. However, at 4 days and 7 days after SE, both VEGFR-3 and VEGF-C immunoreactivities were observed mainly in astrocytes and in some microglia of the stratum radiatum and lacunosum-moleculare of the hippocampus, respectively. These data indicate that VEGF-C and VEGFR-3 can be upregulated in hippocampal astrocytes and microglia after pilocarpine-induced SE, providing basic information about VEGF-C and VEGFR-3 expression patterns following acute seizures.

INTRODUCTION

Temporal lobe epilepsy (TLE), one of the most common adult focal epilepsies, can induce a variety of molecular changes in many brain regions [1,2]. Histologically, TLE is characterized by hippocampal neuronal damage, glial cell activation, angiogenesis, and sprouting of mossy fibers [3-6]. To recapitulate key findings of TLE in rodents, systemic administration of pilocarpine, a muscarinic agonist, is frequently used [7]. Pilocarpine injection can result in status epilepticus (SE), which is associated with neuronal cell loss and reactive gliosis [8-11]. Although several cellular changes in the hippocampus have been reported after pilocarpine-induced SE, essential pathophysiologic mechanisms are still not fully appreciated. Thus, more extensive investigation is warranted to identify key molecular candidates that are altered after acute seizures.

Vascular endothelial growth factor (VEGF)-C belongs to the VEGF family, which consists of 7 different members, VEGF-A,

Author contributions: S.Y.K. and M.Y.L. conceived and designed the experiments. J.Y.K. and K.H.J. performed the experiments. K.O.C. analyzed the data and wrote the manuscript.

VEGF-B, VEGF-C, VEGF-D, VEGF-E, VEGF-F, and placental growth factor [12]. These ligands specifically bind to transmembrane receptor tyrosine kinases including VEGF receptor-1 (VEGFR-1), VEGF receptor-2 (VEGFR-2), and VEGF receptor-3 (VEGFR-3) with different affinity and selectivity [12]. VEGFR-3, also known as Fms-related tyrosine kinase 4 (FLT4), can be activated by VEGF-C, which plays a critical role in lymphangiogenesis [12-14]. In the central nervous system, VEGF-C and its receptor VEGFR-3 are widely expressed in developing and adult brains [15-18]. Ischemic stroke can enhance expression of VEGF-C and VEGFR-3 in various cell types, including neural progenitors, immature neurons, astrocytes, microglia, and perivascular cells, suggesting the versatile roles of VEGF-C/VEGFR-3 signaling after brain insults [19-22].

Interestingly, several papers reported increased expression of VEGF-C and VEGFR-3 in the brains of patients with epilepsy [23-25]. Moreover, when all three VEGF receptors were inhibited by sunitinib after acute seizures, spontaneous recurrent seizures were not observed compared to controls who generated recurrent seizures within one week post-pilocarpine [26]. These pieces of evidence suggest that the VEGF-C/VEGFR-3 signaling may play an important role in epilepsy. However, the results from human epileptic tissues could only provide cross-sectional examination of VEGF-C and VEGFR-3 expressions without comprehensive expression patterns. For this reason, we investigated the spatiotemporal expression of VEGF-C and VEGFR-3 in the hippocampus using a mouse model of epilepsy. We also examined phenotypes of VEGF-C- and VEGFR-3-expressing cells after pilocarpine-induced SE.

METHODS

Animals

Male C57BL/6N mice (8 weeks old; Koatech, Pyeongtaek, Korea) were housed at a standard temperature (22°C ± 1°C) in a light-controlled environment (light on from 8:00 AM to 8:00 PM) with food and water *ad libitum*. Animal experiments were approved by the Ethics Committee of the Catholic University of Korea (approval number: CUMS-2013-0069-02) and were carried out in accordance with the National Institutes of Health Guide for the Care and Use of Laboratory Animals (NIH publication no. 80–23, revised 1996).

Pilocarpine-induced status epilepticus

The pilocarpine-induced SE model was established as previously described [27-29]. Briefly, mice were administrated atropine methyl nitrate (2 mg/kg, i.p.; Tokyo Chemical Industry Co., Tokyo, Japan) and terbutaline hemisulfate salt (2 mg/kg, i.p.; Sigma-Aldrich, St. Louis, MO, USA) 30 min before injection of pilocarpine hydrochloride (280 mg/kg, i.p.; Sigma-Aldrich). After pilocarpine administration, mice were closely monitored for approximately 3 h to evaluate the severity and length of behavioral seizures. Seizure stage was determined according to the Racine scale [30]: stage 1, facial clonus; stage 2, head nodding; stage 3, forelimb clonus; stage 4, rearing; and stage 5, rearing and falling. Animals that had continuous generalized convulsive seizures (stages 3–5) were considered to show SE and were selected for further studies. After 2 h of SE, diazepam (10 mg/kg, i.p.) was administered to quell seizures. To facilitate recovery, all experimental animals were given water-moistened chow and housed in an incubator (30°C ± 1°C) for 5 days until they could maintain a stable body temperature. Then, they were returned to their original cages until they were sacrificed.

Tissue preparation

Brains were collected at 1, 4, and 7 days after SE onset. At each time point, mice were deeply anesthetized by 15% chloral hydrate and transcardially perfused with saline followed by 4% paraformaldehyde in 0.1 M phosphate buffer (PB, pH 7.4). After brains were isolated, they were post-fixed in paraformaldehyde for 24 h and dehydrated with 30% sucrose solution for 3 days. Brains were embedded in Tissue-Tek (Sakura Finetechnical, Tokyo, Japan) for cryoprotection and were rapidly frozen with liquid nitrogen. Using a cryostat, 20 μm thick serial sections were cut coronally at every 5th section at an interval of 80 μm (total 400 μm, between –1.58 and –1.98 from bregma) and were further processed for staining (n = 6 per group).

Fluoro-Jade staining

Tissue sections were mounted to gelatin-coated slides and treated with 0.06% potassium permanganate for 7 min at room temperature. After washing with distilled water, sections were transferred to 0.001% Fluoro-Jade solution for 30 min with gentle shaking. Then, the sections were dried for 1 h and dehydrated through a series of ethanol and 100% xylene. Finally, the sections were mounted with dibutylphthalate polystyrene xylene and observed using fluorescence microscopy (Axioimager M1; Carl Zeiss, Jena, Germany).

Immunohistochemistry

Tissue sections were incubated with 3% H_2O_2 and 10% methanol in 0.01 M phosphate buffered saline (PBS; Sigma-Aldrich) to destroy endogenous peroxidase activities. Next, sections were blocked with 10% normal goat serum in 0.01 M PBS for 1 h and then incubated overnight at 4°C with antibodies to VEGF-C (1:500; Santa Cruz Biotechnology, Santa Cruz, CA, USA), VEGFR-3 (1:500; Abnova, Taipei, Taiwan), glial fibrillary acidic protein (GFAP, 1:400; Chemicon International Inc., Temecula,

CA, USA), or Ox42 (1:100; Serotec, Oxford, UK). On the next day, sections were incubated with anti-rabbit immunoglobulin G (IgG) (1:200), anti-mouse IgG (1:500), or anti-rat IgG (1:500) for 2 h at room temperature. Finally, the sections were visualized with 0.1% diaminobenzidine tetrahydrochloride and 0.005% H_2O_2 in 0.05 M Tris HCl (pH 7.4) and observed using a light microscope (BX51; Olympus, Tokyo, Japan).

For triple labeling, the sections were incubated with rabbit anti-VEGF-C or VEGFR-3 (1:500), mouse anti-GFAP (1:400), and rat anti-Ox42, followed by Cy3- (1:500; Jackson ImmunoResearch, West Grove, PA, USA), Cy5- (1:500; Jackson ImmunoResearch), and Alexa fluor 488-conjugated IgG (1:300; Invitrogen, Carlsbad, CA, USA), respectively. Finally, sections were mounted and observed using a confocal microscope (LSM 510 Meta; Carl Zeiss).

Quantitative analysis of VEGF-C- and VEGFR-3-expressing cells

Five coronal sections in the hippocampus of 6 sham-treated animals, and animals at 1, 4, and 7 days post-pilocarpine treatment (6 animals per each time-point) were obtained with an interval of 80 μm. Cell counting was performed as described previously [27], with slight modifications. The number of VEGF-C, VEGFR-3, VEGF-C/GFAP, VEGF-C/Ox42, VEGFR-3/GFAP, or VEGFR-3/Ox42 immunoreactive cells in the hippocampus was counted in the area covering the stratum radiatum and lacunosum-moleculare. To quantify VEGF-C and VEGFR-3 expression after SE, the total number of immunoreactive cells in 5 sections was counted using ZEN image examiner software (Zen 2009; Carl Zeiss). Regarding analysis of double-labeled cells, the percentages of VEGF-C/GFAP and VEGF-C/Ox42 double-positive cells and GFAP- and Ox42-positive cells were calculated. In addition, the total number of VEGFR-3/GFAP and VEGFR-3/Ox42 immunoreactive cells

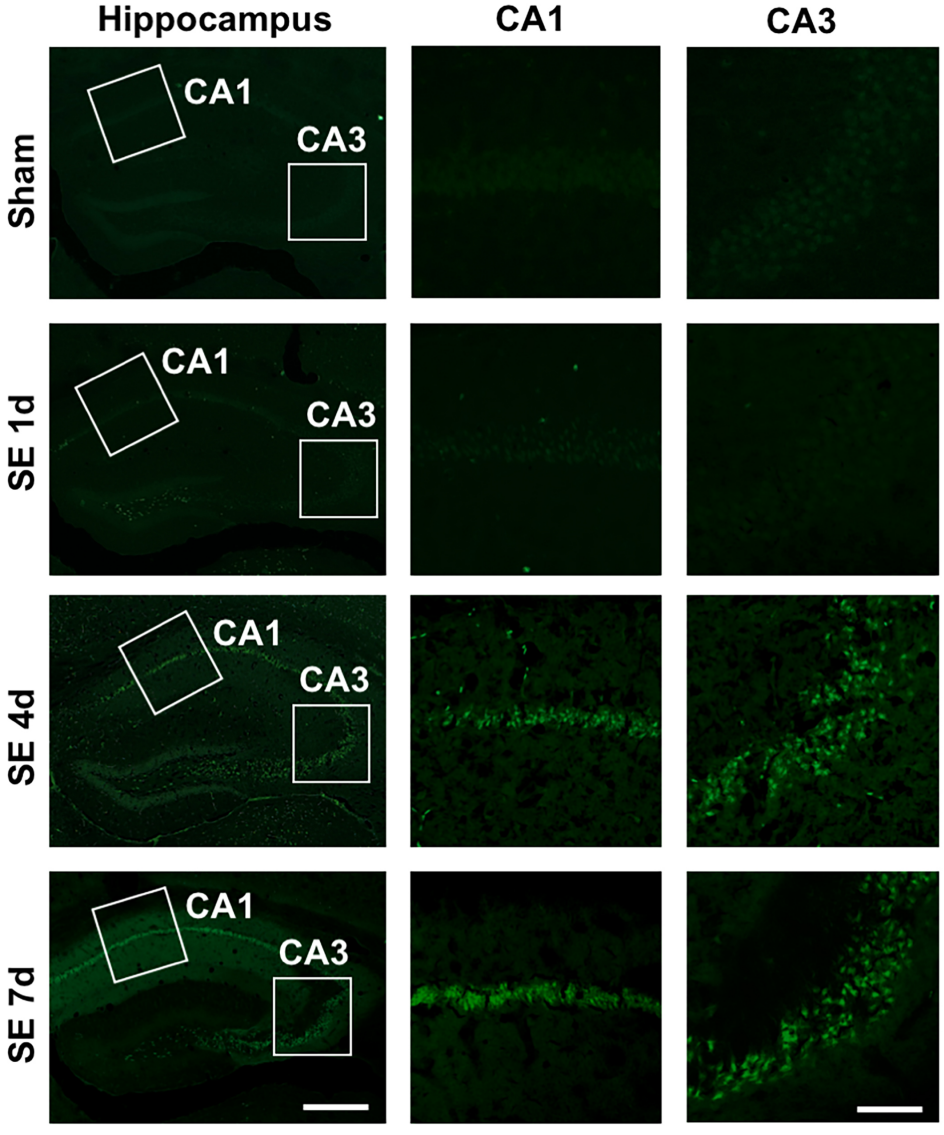

Fig. 1. Temporal profiles of neuronal death assessed by Fluoro-Jade staining in the hippocampus following pilocarpine injection. Compared to sham-manipulated hippocampi with no Fluoro-Jade positive neurons, at 1 day after pilocarpine-induced status epilepticus (SE), hilar neurons started to express Fluoro-Jade reactivity. At 4 days and 7 days after pilocarpine-induced SE, a number of Fluoro-Jade positive pyknotic cells were observed in CA1 and CA3 subfields of the hippocampus, representing degenerating neurons. Scale bar in far left column = 200 μm; same magnification was used for photomicrographs labeled as hippocampus. Scale bar in far right column = 50 μm; same magnification was used for photomicrographs labeled as CA1 and CA3. N = 6 per each time-point.

was divided by the total number of GFAP or Ox42 positive cells, respectively, to provide the cellular profiles of VEGFR-3 expression after acute seizures.

Statistical analysis

Data are presented as the mean ± standard error of the mean. Statistical significance was assessed using GraphPad Prism 7 software (GraphPad Software Inc., San Diego, CA, USA). One-way analysis of variance (ANOVA) was performed to compare the number of VEGF-C- and VEGFR-3-expressing cells and was followed by Dunnett's *post-hoc* test. A value of $p < 0.05$ was considered statistically significant.

RESULTS

Neuronal cell death after pilocarpine-induced SE

To analyze neuronal death after acute seizures, Fluoro-Jade staining was performed to detect degenerating neurons (Fig. 1). There were no Fluoro-Jade-positive cells in sham-manipulated controls. However, at 1 day after pilocarpine injection, hilar neurons started to show Fluoro-Jade reactivity while pyramidal neurons were not marked by Fluoro-Jade staining. At 4 days after SE onset, Fluoro-Jade stained pyramidal neurons were clearly detected in medial CA1 and CA3 subfields of the hippocampus in addition to hilar region of the dentate gyrus. This was consistently observed at 7 days after SE onset. These data indicate that pilocarpine-induced SE can result in neuronal death, confirming that our model was reliable and reproducible.

Reactive hippocampal gliosis after pilocarpine-induced SE

Since pilocarpine-induced SE can activate glial cells in the hippocampus, immunoreactivities to GFAP (astrocyte marker) and Ox42 (microglia marker) were examined (Fig. 2). Compared to sham-manipulated animals, where few GFAP- and Ox42-immunoreactive cells were found in the hippocampus, animals

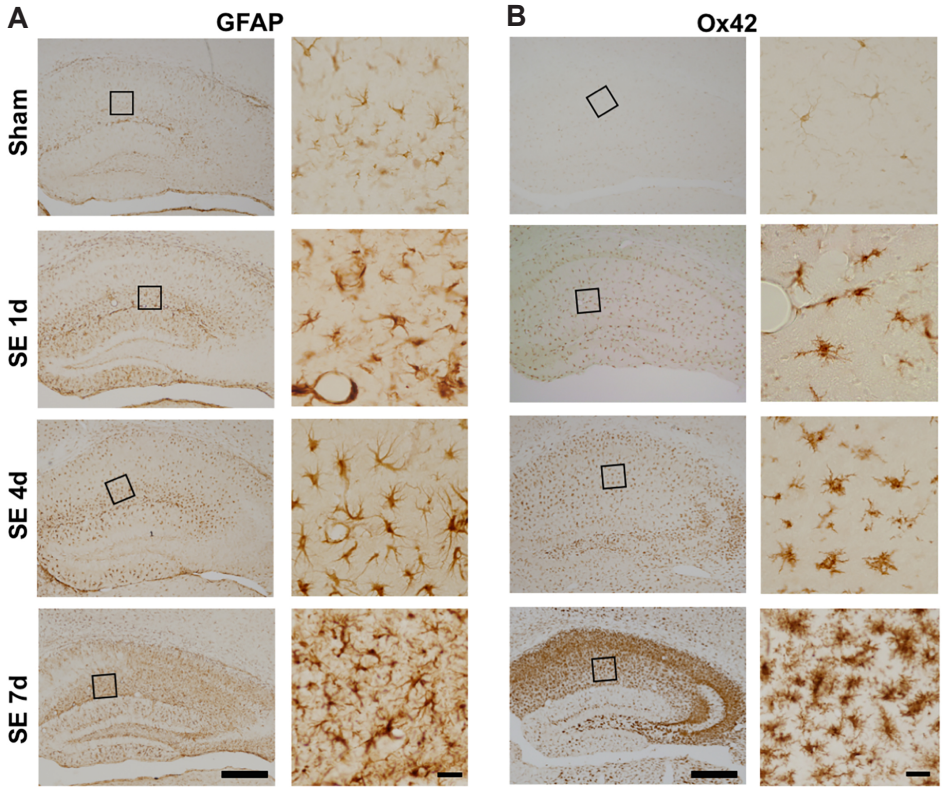

Fig. 2. Temporal profiles of reactive gliosis in hippocampus following pilocarpine injection. (A) Immunohistochemistry for glial fibrillary acidic protein (GFAP) showed increased GFAP immunoreactivity at 1 day after status epilepticus (SE) onset and further elevation at 4 days and 7 days after pilocarpine-induced SE, whereas minimal GFAP expression was observed in sham-manipulated animals. A square in each low magnification photomicrograph was visualized in the next panel. Scale bar in bottom left column = 200 μm; same magnification was used for entire left column. Scale bar in bottom right column = 20 μm; same magnification was used for entire right column. N = 6 per each time-point. (B) Immunohistochemistry for Ox42 showed markedly increased Ox42 immunoreactivity from 1 day after SE compared to sham-manipulated animals. A square in each low magnification photomicrograph was visualized in the next panel. Scale bar in bottom left column = 200 μm; same magnification was used for entire left column. Scale bar in bottom right column = 20 μm; same magnification was used for entire right column. N = 6 per each time-point.

who experienced acute seizures by pilocarpine injection showed increased numbers of GFAP- and Ox42-expressing cells in addition to hypertrophic morphology.

Spatiotemporal expression of VEGF-C and VEGFR-3 after pilocarpine-induced SE

After confirming our mouse model of epilepsy, the temporal pattern of VEGF-C and VEGFR-3 expression in the hippocampus was examined with immunohistochemistry (Fig. 3). In sham-manipulated animals, VEGF-C was mainly expressed in pyramidal neurons of the hippocampus and a few cells in the subpyramidal zone (Fig. 3A). Although VEGF-C expression at 1 day after SE was similar to that of the sham group, VEGF-C immunoreactivity was markedly increased in relatively small cells in the subpyramidal zone at 4 days and 7 days after SE (Fig. 3A). Immunoreactivity to VEGFR-3 was mainly observed in pyramidal cells of the hippocampus in sham-manipulated animals (Fig. 3A). Similar to VEGF-C expression after acute seizures, VEGFR-3-positive cells were remarkably increased in the subpyramidal zone of the hippocampus at 4 days and 7 days after SE onset (Fig. 3A). When VEGF-C- and VEGFR-3-expressing cells were quantitatively analyzed in the subpyramidal zone (Fig. 3B), the numbers of both VEGF-C- and VEGFR-3-immunoreactive cells were significantly increased at 4 days and 7 days after pilocarpine-induced SE compared to sham-controls (Fig. 3C, D). Conversely, VEGF-C- and VEGFR-3-expressing pyramidal neurons began to disappear at 4 days post-pilocarpine and notably decreased at 7 days after SE, possibly due to neuronal death induced by pilocarpine-induced SE.

Cellular phenotypes of VEGF-C and VEGFR-3 expression after pilocarpine-induced SE

Because the morphology of VEGF-C- or VEGFR-3-immunoreactive cells after SE was consistent with glial cells, triple immunofluorescence with GFAP, Ox42, and either VEGF-C or VEGFR-3 was carried out to identify the phenotypes of VEGF-C- or VEGFR-3-expressing cells (Figs. 4 and 5). Since VEGF-C and VEGFR-3 expression peaked at 7 days and 4 days after SE, respec-

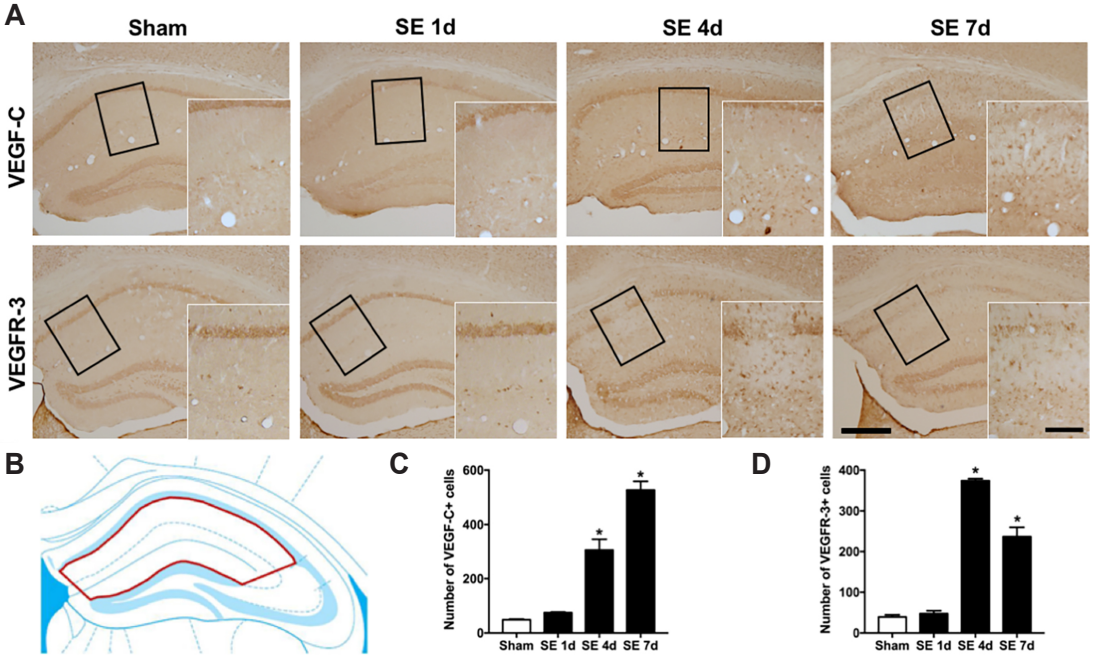

Fig. 3. Spatiotemporal profiles of vascular endothelial growth factor (VEGF)-C and vascular endothelial growth factor receptor (VEGFR)-3 immunoreactivity after pilocarpine-induced status epilepticus (SE). (A) Immunoreactivity to VEGF-C and VEGFR-3 was observed in pyramidal cell layer and granule cells in the hippocampus of sham-manipulated animals. However, from 1 day after SE, small cells in the statum radiatum started to express VEGF-C and VEGFR-3, which was enhanced at 4 days and 7 days after pilocarpine-induced SE. A rectangle in each low magnification photomicrograph is visualized in the inset. Scale bar in bottom left of VEGFR-3-stained image at 7 days after SE = 200 μm; same magnification was used for all lower magnification photomicrographs. Scale bar in bottom right of VEGFR-3-stained inset at 7 days after SE = 50 μm; same magnification was used for all insets. (B) Schematic indicating the subpyramidal zone where VEGF-C- and VEGFR-3-expressing cells were quantitatively analyzed. (C) Graph showing number of VEGF-C-immmnoreactive cells in subpyramidal zone. VEGF-C-positive cells were significantly increased at 4 days after SE and peaked at 7 days after SE compared to sham-controls. Values are expressed as mean ± standard error of the mean (SEM). One-way analysis of variance (ANOVA) followed by Dunnett's *post-hoc* test was performed. N = 6 for each group, *p < 0.05 *vs.* sham. (D) Graph showing number of VEGFR-3 immmnoreactive cells in subpyramidal zone. VEGFR-3 positive cells were significantly increased at 4 days and 7 days after SE compared to sham-controls. Values are expressed as mean ± SEM. One-way ANOVA followed by Dunnett's *post-hoc* test was performed. N = 6 mice for each group, *p < 0.05 *vs.* sham.

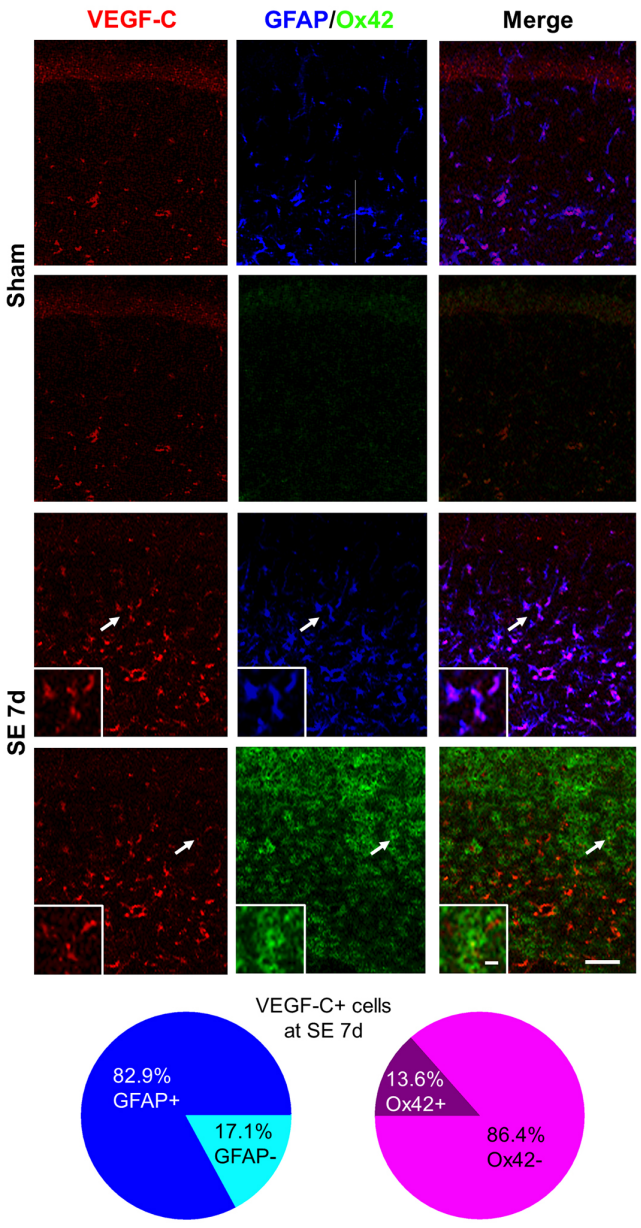

Fig. 4. Phenotypic analysis of vascular endothelial growth factor (VEGF)-C immunoreactive cells in hippocampus following pilocarpine injection. In sham-manipulated animals, most VEGF-C-positive cells were pyramidal neurons and a few glial fibrillary acidic protein (GFAP)-colabeled astrocytes in the stratum radiatum, without Ox42 co-labeled microglia. At 7 days after status epilepticus (SE), VEGF-C positive cells co-expressed GFAP or Ox42 immunoreactivity in the subpyramidal zone of the hippocampus. White arrows indicate double-labeled cells magnified in the insets. Among GFAP expressing cells in the subpyramidal zone, 82.9% showed VEGF-C immunoreactivity, whereas 13.6% of all Ox42 positive cells demonstrated VEGF-C expression. Scale bar = 50 μm for low magnified images. Scale bar = 10 μm for insets. N = 6 per each group.

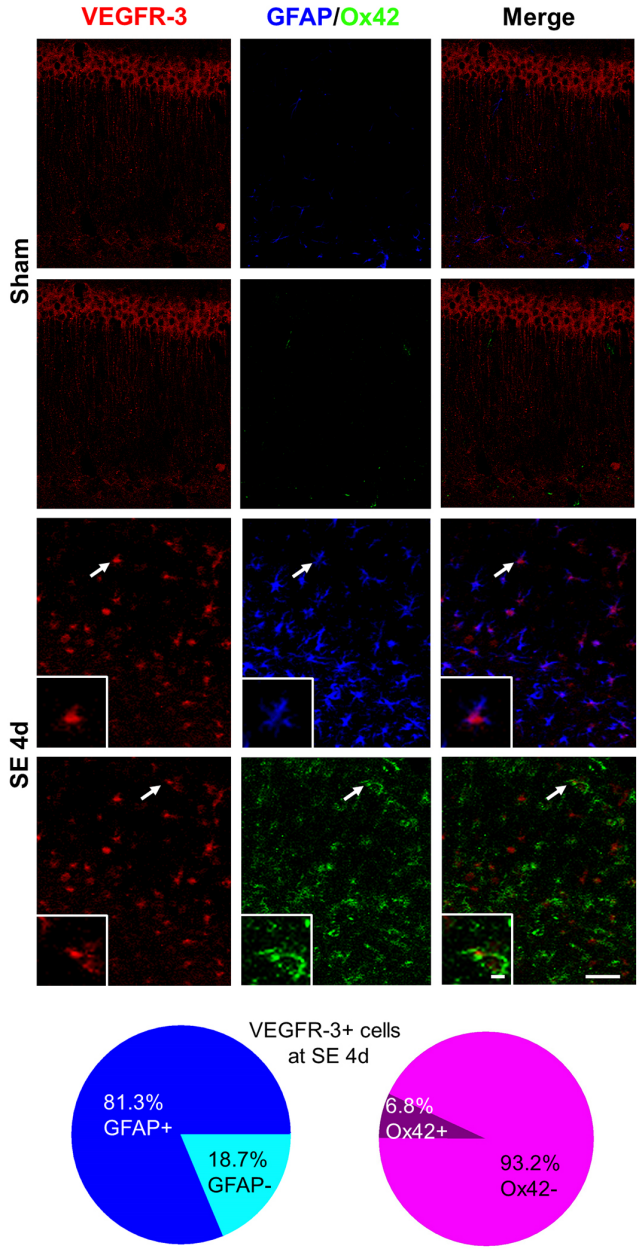

Fig. 5. Phenotypic analysis of vascular endothelial growth factor receptor (VEGFR)-3 immunoreactive cells in hippocampus following pilocarpine injection. In sham-manipulated animals, VEGFR-3 positive cells were pyramidal neurons without glial fibrillary acidic protein (GFAP) or Ox42 expressing glial cells. At 4 days after status epilepticus (SE), VEGFR-3 positive cells co-expressed GFAP or Ox42 immunoreactivity in the subpyramidal zone of the hippocampus. White arrows indicate a representative double-labeled cell magnified in the insets. Among GFAP expressing cells in subpyramidal zone, 81.3% showed VEGFR-3 immunoreactivity, whereas 6.8% of all Ox42 positive cells demonstrated VEGFR-3 expression. Scale bar = 50 μm for low magnified images. Scale bar = 10 μm for insets. N = 6 per each group.

tively, hippocampal sections at each time-point were selected for cellular phenotype analysis. In sham-manipulated animals, most VEGF-C immunoreactivity was found in neurons (Fig. 4). Moreover, there were a few VEGF-C labeled cells in the subpyramidal zone that co-labeled with GFAP (Fig. 4). However, at 7 days after SE, 82.9% of GFAP-positive cells were VEGF-C/GFAP double-labeled astrocytes and 13.6% of Ox42-expressing cells were VEGF-C/Ox42 double-positive microglial cells (Fig. 4). There

was no glial expression of VEGFR-3 in sham-controls. However, at 4 days after SE, 81.3% of GFAP-immunoreactive cells were VEGFR-3/GFAP double-labeled astrocytes and 6.8% of Ox42-expressing cells were VEGFR-3/Ox42 double-positive microglia (Fig. 5), similar to VEGF-C expression. These data demonstrated that VEGF-C and VEGFR-3 protein were primarily expressed in neuronal cells under physiologic conditions, but after prolonged seizure activities, the expression of VEGF-C and VEGFR-3 was more prominent in reactive astrocytes.

DISCUSSION

The present study demonstrates that VEGF-C and VEGFR-3 are significantly upregulated in the hippocampus after pilocarpine-induced SE. Both VEGF-C and its receptor, VEGFR-3, are activated at 4 days and 7 days after SE, in parallel with pyramidal neuronal death. VEGF-C- and VEGFR-3 immunoreactive cells induced by SE are mainly reactive astrocytes and a few microglial cells.

Physiologically, VEGF-C and VEGFR-3 have been a critical regulator of lymphangiogenesis [12-14]. In the central nervous system, many researchers including us demonstrated VEGF-C/VEGFR-3 expressions in the developing and adult brain [15-18,31]. Consistent with previous reports, we also observed VEGF-C and VEGFR-3 immunoreactivities mainly in the pyramidal neurons and granule cells, in addition to several other cell types in the hippocampus. With regard to the function of VEGF-C/VEGFR-3 in the brain, blocking VEGFR-3 in retinal microvessels could inhibit angiogenic sprouting and branching [32], suggesting that VEGFR-3 can mediate the fine tuning of vessel branching. Moreover, VEGF-C and VEGFR-3 could promote neurogenesis in the hippocampus and the subventricular zone by modulating the proliferation of neural stem cells [33,34]. Furthermore, glial progenitors were also influenced by VEGF-C/VEGFR-3 signaling [35,36], suggesting versatile roles of VEGF-C and VEGFR-3. Thus, it will be interesting to examine diverse cell types expressing VEGF-C and VEGFR-3 in the brain and their impact on homeostatic regulation of cytogenesis.

A number of studies have reported that epilepsy is characterized by neuronal cell death and reactive glial responses in several brain regions [37-39]. Pilocarpine-induced SE is a reliable model used to study the pathophysiologic mechanisms of epilepsy because it reproduces electrographic, histologic, and behavioral alterations of epilepsy [8,10,40]. Fluoro-Jade staining demonstrated pyramidal neuronal death in addition to hilar neuronal damage after pilocarpine injection. Moreover, GFAP-expressing astrocytes and Ox42-immunoreactive microglia became hypertrophic with thick bundles of glial filaments within 1 day after SE, corroborating that our model system is in line with other studies [9,11].

VEGF-C and VEGFR-3 are upregulated in various diseases, including myocardial infarction, experimental autoimmune encephalomyelitis, ischemic stroke, and epilepsy [19-25,41,42]. Consistent with previous results, our immunohistochemistry results showed increased VEGF-C and VEGFR-3 expressing cells in the hippocampus after acute seizures. Temporal expression profiling further revealed that these cells began to increase at 4 days after pilocarpine-induced SE, which is a subacute phase in epilepsy. Because blockade of activation of all three VEGF receptors by sunitinib for 14 days during the subacute phases suppresses spontaneous recurrent seizures [26], targeting the VEGF-C/VEGFR-3 signaling pathway with more specific inhibitors may uncover novel roles of VEGF-C and VEGFR-3 in epilepsy. VEGF-C/VEGFR-3-mediated functions may be related to seizure-induced aberrant neurogenesis and/or neuroprotection. Since VEGF-C promotes dentate and subventricular neurogenesis via VEGFR-3 [33-35], increased VEGF-C after acute seizures may enhance proliferation of neural progenitors in the hippocampus, which can result in increased ectopic granule cells. Considering that aberrant hippocampal neurogenesis can contribute to the generation of chronic seizures [43], blockade of the VEGF-C/VEGFR-3 signaling pathway may reduce recurrent seizures. Another plausible role of VEGF-C and VEGFR-3 is neuroprotection. In our previous report, we showed that ischemic preconditioning increased VEGF-C expression in pyramidal neurons. When a specific VEGFR-3 inhibitor, SAR131675, was administered, the neuroprotective effects of ischemic preconditioning were abolished, suggesting involvement of the VEGF-C/VEGFR-3 pathway in ischemic tolerance [44]. As the general molecular mechanisms that follow brain insults are considered to be similar for ischemia and epilepsy [45], it is possible that increased VEGF-C and VEGFR-3 expression after acute seizures may be an attempt to promote endogenous neuroprotection. Further studies modifying VEGF-C or VEGFR-3 expression are required to elucidate the specific roles of VEGF-C/VEGFR-3 signaling in epilepsy.

VEGF-C and VEGFR-3 were originally identified as major regulators of lymphangiogenesis [13,14,46]. The main lymphatic vessels in the brain are located in the dura and drain cerebrospinal fluids (CSF) to deep cervical lymph nodes [47]. However, it remains unclear how interstitial fluids in the brain parenchyma drain to the meningeal lymphatic vessels. Although controversial, one interesting hypothesis is that astrocytes are critical to clearing interstitial macroscopic solutes by utilizing the water channel aquaporin-4 [48,49]. Our study showed that most reactive astrocytes in the hippocampus expressed VEGF-C and VEGFR-3, which are essential molecules in regulation of lymphatics. Therefore, astrocytic VEGF-C secreted to the interstitial space of the hippocampus may be dispersed to CSF or veins to stimulate the formation of meningeal lymphatic vessels, eventually enhancing drainage of parenchymal waste to the dural lymphatics. Seizure-induced dysfunction of the blood-brain barrier generates a massive influx of blood-driven serum proteins such as albumin, which lowers the seizure threshold [50]. It will be interesting to

elucidate the unequivocal roles of glial VEGF-C and VEGFR-3 in association with clearance of soluble wastes.

In conclusion, we provided the spatiotemporal expression pattern of VEGF-C and VEGFR-3 in the hippocampus after pilocarpine-induced SE. We also showed that the main cell type responsible for increased VEGF-C and VEGFR-3 after acute seizures is astrocytes, in addition to a few microglia. Our results provide a scientific basis for the role of the VEGF-C/VEGFR-3 pathway in epileptic seizures.

ACKNOWLEDGEMENTS

We thank Mr. Jae-Cheon Kim for his technical support. This work was supported by National Research Foundation of Korea (NRF) grants funded by the Korean government (NRF-2017R1A2B4002704 to S.Y.K. and NRF-2019K2A9A2A08000167 to K.O.C.).

CONFLICTS OF INTEREST

The authors declare no conflicts of interest.

REFERENCES

1. Lehéricy S, Semah F, Hasboun D, Dormont D, Clémenceau S, Granat O, Marsault C, Baulac M. Temporal lobe epilepsy with varying severity: MRI study of 222 patients. *Neuroradiology.* 1997;39:788-796.
2. Howe KL, Dimitri D, Heyn C, Kiehl TR, Mikulis D, Valiante T. Histologically confirmed hippocampal structural features revealed by 3T MR imaging: potential to increase diagnostic specificity of mesial temporal sclerosis. *AJNR Am J Neuroradiol.* 2010;31:1682-1689.
3. Cronin J, Dudek FE. Chronic seizures and collateral sprouting of dentate mossy fibers after kainic acid treatment in rats. *Brain Res.* 1988;474:181-184.
4. de Lanerolle NC, Kim JH, Robbins RJ, Spencer DD. Hippocampal interneuron loss and plasticity in human temporal lobe epilepsy. *Brain Res*. 1989;495:387-395.
5. Sutula T, Cascino G, Cavazos J, Parada I, Ramirez L. Mossy fiber synaptic reorganization in the epileptic human temporal lobe. *Ann Neurol.* 1989;26:321-330.
6. Maglóczky Z, Wittner L, Borhegyi Z, Halász P, Vajda J, Czirják S, Freund TF. Changes in the distribution and connectivity of interneurons in the epileptic human dentate gyrus. *Neuroscience.* 2000;96:7-25.
7. Buckmaster PS, Haney MM. Factors affecting outcomes of pilocarpine treatment in a mouse model of temporal lobe epilepsy. *Epilepsy Res.* 2012;102:153-159.
8. Turski WA, Cavalheiro EA, Bortolotto ZA, Mello LM, Schwarz M, Turski L. Seizures produced by pilocarpine in mice: a behavioral, electroencephalographic and morphological analysis. *Brain Res.* 1984;321:237-253.
9. Cavalheiro EA. The pilocarpine model of epilepsy. *Ital J Neurol Sci.* 1995;16:33-37.
10. Turski WA, Cavalheiro EA, Schwarz M, Czuczwar SJ, Kleinrok Z, Turski L. Limbic seizures produced by pilocarpine in rats: behavioural, electroencephalographic and neuropathological study. *Behav Brain Res.* 1983;9:315-335.
11. Borges K, Gearing M, McDermott DL, Smith AB, Almonte AG, Wainer BH, Dingledine R. Neuronal and glial pathological changes during epileptogenesis in the mouse pilocarpine model. *Exp Neurol.* 2003;182:21-34.
12. Yamazaki Y, Morita T. Molecular and functional diversity of vascular endothelial growth factors. *Mol Divers.* 2006;10:515-527.
13. Saharinen P, Tammela T, Karkkainen MJ, Alitalo K. Lymphatic vasculature: development, molecular regulation and role in tumor metastasis and inflammation. *Trends Immunol.* 2004;25:387-395.
14. Oliver G. Lymphatic vasculature development. *Nat Rev Immunol.* 2004;4:35-45.
15. Lagercrantz J, Farnebo F, Larsson C, Tvrdik T, Weber G, Piehl F. A comparative study of the expression patterns for vegf, vegf-b/vrf and vegf-c in the developing and adult mouse. *Biochim Biophys Acta.* 1998;1398:157-163.
16. Ward MC, Cunningham AM. Developmental expression of vascular endothelial growth factor receptor 3 and vascular endothelial growth factor C in forebrain. *Neuroscience.* 2015;303:544-557.
17. Choi JS, Shin YJ, Lee JY, Yun H, Cha JH, Choi JY, Chun MH, Lee MY. Expression of vascular endothelial growth factor receptor-3 mRNA in the rat developing forebrain and retina. *J Comp Neurol.* 2010;518:1064-1081.
18. Hou Y, Shin YJ, Han EJ, Choi JS, Park JM, Cha JH, Choi JY, Lee MY. Distribution of vascular endothelial growth factor receptor-3/Flt4 mRNA in adult rat central nervous system. *J Chem Neuroanat.* 2011;42:56-64.
19. Shin YJ, Choi JS, Lee JY, Choi JY, Cha JH, Chun MH, Lee MY. Differential regulation of vascular endothelial growth factor-C and its receptor in the rat hippocampus following transient forebrain ischemia. *Acta Neuropathol.* 2008;116:517-527.
20. Shin YJ, Choi JS, Choi JY, Hou Y, Cha JH, Chun MH, Lee MY. Induction of vascular endothelial growth factor receptor-3 mRNA in glial cells following focal cerebral ischemia in rats. *J Neuroimmunol.* 2010;229:81-90.
21. Shin YJ, Choi JS, Choi JY, Cha JH, Chun MH, Lee MY. Enhanced expression of vascular endothelial growth factor receptor-3 in the subventricular zone of stroke-lesioned rats. *Neurosci Lett.* 2010;469:194-198.
22. Shin YJ, Park JM, Cho JM, Cha JH, Kim SY, Lee MY. Induction of vascular endothelial growth factor receptor-3 expression in perivascular cells of the ischemic core following focal cerebral ischemia in rats. *Acta Histochem.* 2013;115:170-177.
23. Zhang CQ, Shu HF, Yin Q, An N, Xu SL, Yin JB, Song YC, Liu SY, Yang H. Expression and cellular distribution of vascular endothelial growth factor-C system in cortical tubers of the tuberous sclerosis complex. *Brain Pathol.* 2012;22:205-218.
24. Sun FJ, Wei YJ, Li S, Guo W, Chen X, Liu SY, He JJ, Yin Q, Yang H, Zhang CQ. Elevated expression of VEGF-C and its receptors, VEGFR-2 and VEGFR-3, in patients with mesial temporal lobe epilepsy. *J*

Mol Neurosci. 2016;59:241-250.
25. Castañeda-Cabral JL, Beas-Zárate C, Rocha-Arrieta LL, Orozco-Suárez SA, Alonso-Vanegas M, Guevara-Guzmán R, Ureña-Guerrero ME. Increased protein expression of VEGF-A, VEGF-B, VEGF-C and their receptors in the temporal neocortex of pharmacoresistant temporal lobe epilepsy patients. *J Neuroimmunol.* 2019;328:68-72.
26. Benini R, Roth R, Khoja Z, Avoli M, Wintermark P. Does angiogenesis play a role in the establishment of mesial temporal lobe epilepsy? *Int J Dev Neurosci*. 2016;49:31-36.
27. Jeong KH, Lee KE, Kim SY, Cho KO. Upregulation of Krüppel-like factor 6 in the mouse hippocampus after pilocarpine-induced status epilepticus. *Neuroscience.* 2011;186:170-178.
28. Jang HJ, Kim JE, Jeong KH, Lim SC, Kim SY, Cho KO. The neuroprotective effect of hericium erinaceus extracts in mouse hippocampus after pilocarpine-induced status epilepticus. *Int J Mol Sci.* 2019;20:859.
29. Kim JE, Cho KO. The pilocarpine model of temporal lobe epilepsy and EEG monitoring using radiotelemetry system in mice. *J Vis Exp.* 2018;(132):56831.
30. Racine RJ. Modification of seizure activity by electrical stimulation. II. Motor seizure. *Electroencephalogr Clin Neurophysiol.* 1972; 32:281-294.
31. Hou Y, Choi JS, Shin YJ, Cha JH, Choi JY, Chun MH, Lee MY. Expression of vascular endothelial growth factor receptor-3 mRNA in the developing rat cerebellum. *Cell Mol Neurobiol.* 2011;31:7-16.
32. Tammela T, Zarkada G, Wallgard E, Murtomäki A, Suchting S, Wirzenius M, Waltari M, Hellström M, Schomber T, Peltonen R, Freitas C, Duarte A, Isoniemi H, Laakkonen P, Christofori G, Ylä-Herttuala S, Shibuya M, Pytowski B, Eichmann A, Betsholtz C, et al. Blocking VEGFR-3 suppresses angiogenic sprouting and vascular network formation. *Nature.* 2008;454:656-660.
33. Han J, Calvo CF, Kang TH, Baker KL, Park JH, Parras C, Levittas M, Birba U, Pibouin-Fragner L, Fragner P, Bilguvar K, Duman RS, Nurmi H, Alitalo K, Eichmann AC, Thomas JL. Vascular endothelial growth factor receptor 3 controls neural stem cell activation in mice and humans. *Cell Rep.* 2015;10:1158-1172.
34. Calvo CF, Fontaine RH, Soueid J, Tammela T, Makinen T, Alfaro-Cervello C, Bonnaud F, Miguez A, Benhaim L, Xu Y, Barallobre MJ, Moutkine I, Lyytikkä J, Tatlisumak T, Pytowski B, Zalc B, Richardson W, Kessaris N, Garcia-Verdugo JM, Alitalo K, et al. Vascular endothelial growth factor receptor 3 directly regulates murine neurogenesis. *Genes Dev.* 2011;25:831-844.
35. Le Bras B, Barallobre MJ, Homman-Ludiye J, Ny A, Wyns S, Tammela T, Haiko P, Karkkainen MJ, Yuan L, Muriel MP, Chatzopoulou E, Bréant C, Zalc B, Carmeliet P, Alitalo K, Eichmann A, Thomas JL. VEGF-C is a trophic factor for neural progenitors in the vertebrate embryonic brain. *Nat Neurosci.* 2006;9:340-348.
36. Kranich S, Hattermann K, Specht A, Lucius R, Mentlein R. VEGFR-3/Flt-4 mediates proliferation and chemotaxis in glial precursor cells. *Neurochem Int.* 2009;55:747-753.
37. Morimoto K, Fahnestock M, Racine RJ. Kindling and status epilepticus models of epilepsy: rewiring the brain. *Prog Neurobiol.* 2004; 73:1-60.
38. Scorza FA, Arida RM, Naffah-Mazzacoratti Mda G, Scerni DA, Calderazzo L, Cavalheiro EA. The pilocarpine model of epilepsy: what have we learned? *An Acad Bras Cienc*. 2009;81:345-365.
39. Fabene PF, Merigo F, Galiè M, Benati D, Bernardi P, Farace P, Nicolato E, Marzola P, Sbarbati A. Pilocarpine-induced status epilepticus in rats involves ischemic and excitotoxic mechanisms. *PLoS One.* 2007;2:1105.
40. Cavalheiro EA, Leite JP, Bortolotto ZA, Turski WA, Ikonomidou C, Turski L. Long-term effects of pilocarpine in rats: structural damage of the brain triggers kindling and spontaneous recurrent seizures. *Epilepsia*. 1991;32:778-782.
41. Zhao T, Zhao W, Meng W, Liu C, Chen Y, Gerling IC, Weber KT, Bhattacharya SK, Kumar R, Sun Y. VEGF-C/VEGFR-3 pathway promotes myocyte hypertrophy and survival in the infarcted myocardium. *Am J Transl Res.* 2015;7:697-709.
42. Hsu M, Rayasam A, Kijak JA, Choi YH, Harding JS, Marcus SA, Karpus WJ, Sandor M, Fabry Z. Neuroinflammation-induced lymphangiogenesis near the cribriform plate contributes to drainage of CNS-derived antigens and immune cells. *Nat Commun.* 2019; 10:229.
43. Cho KO, Lybrand ZR, Ito N, Brulet R, Tafacory F, Zhang L, Good L, Ure K, Kernie SG, Birnbaum SG, Scharfman HE, Eisch AJ, Hsieh J. Aberrant hippocampal neurogenesis contributes to epilepsy and associated cognitive decline. *Nat Commun.* 2015;6:6606.
44. Bhuiyan MI, Kim JC, Hwang SN, Lee MY, Kim SY. Ischemic tolerance is associated with VEGF-C and VEGFR-3 signaling in the mouse hippocampus. *Neuroscience.* 2015;290:90-102.
45. Auer RN, Siesjö BK. Biological differences between ischemia, hypoglycemia, and epilepsy. *Ann Neurol.* 1988;24:699-707.
46. Antila S, Karaman S, Nurmi H, Airavaara M, Voutilainen MH, Mathivet T, Chilov D, Li Z, Koppinen T, Park JH, Fang S, Aspelund A, Saarma M, Eichmann A, Thomas JL, Alitalo K. Development and plasticity of meningeal lymphatic vessels. *J Exp Med.* 2017;214:3645-3667.
47. Louveau A, Smirnov I, Keyes TJ, Eccles JD, Rouhani SJ, Peske JD, Derecki NC, Castle D, Mandell JW, Lee KS, Harris TH, Kipnis J. Structural and functional features of central nervous system lymphatic vessels. *Nature.* 2015;523:337-341.
48. Iliff JJ, Wang M, Liao Y, Plogg BA, Peng W, Gundersen GA, Benveniste H, Vates GE, Deane R, Goldman SA, Nagelhus EA, Nedergaard M. A paravascular pathway facilitates CSF flow through the brain parenchyma and the clearance of interstitial solutes, including amyloid β. *Sci Transl Med.* 2012;4:147ra111.
49. Smith AJ, Yao X, Dix JA, Jin BJ, Verkman AS. Test of the 'glymphatic' hypothesis demonstrates diffusive and aquaporin-4-independent solute transport in rodent brain parenchyma. *Elife.* 2017;6:27679.
50. van Vliet EA, Aronica E, Gorter JA. Blood-brain barrier dysfunction, seizures and epilepsy. *Semin Cell Dev Biol.* 2015;38:26-34.